

Available online at www.sciencedirect.com

ScienceDirect

journal homepage: <http://www.elsevier.com/locate/rpor>

Original research article

Determination of inflection points of CyberKnife dose profiles within acceptability criteria of deviations in measurements

Neslihan Sarıgül^a, Fazlı Yağız Yedekçi^b, Mete Yeğiner^b, Fadıl Akyol^b, Haluk Utku^{a,*}

^a Institute of Nuclear Sciences, Hacettepe University, Ankara, Turkey

^b Department of Radiation Oncology, Hacettepe University, Faculty of Medicine, Ankara, Turkey

ARTICLE INFO

Article history:

Received 30 May 2019

Received in revised form

22 August 2019

Accepted 15 October 2019

Available online 12 November 2019

Keywords:

Inflection Point

Gamma evaluation

Dosimetric field size

CyberKnife

ABSTRACT

Aim: The aim of this study was to determine the Inflection Points (IPs) of flattening filter free (FFF) CyberKnife dose profiles for cone-based stereotactic radiotherapy. In addition, dosimetric field sizes were determined.

Background: The increased need for treatment in the early stages of cancer necessitated the treatment of smaller tumors. However, efforts in that direction required the modeling accuracy of the beam. Removal of the flattening filter (FF) from the path of x-ray beam has provided the solution to those efforts, but required a different normalization approach for the beam to ensure the delivery of the dose accurately. As a solution, researchers proposed a normalization factor based on IPs.

Materials and methods: Measurements using microDiamond (PTW 60019), Diode SRS (PTW 60018) and Monte Carlo (MC) calculations of dose profiles were completed at SAD 80 cm and 5 cm depth for 15–60 mm cones. Performance analysis of detectors with respect to MC calculation was carried out. Gamma evaluation method was used to determine achievable acceptability criteria for FFF CyberKnife beams.

Results: Acceptability within (3%–0.5 mm) was found to be an achievable criterion for all dose profile measurements of the cone beams used in this study. To determine the IP, the first and second derivatives of the dose profile were determined via the cubic spline interpolation technique.

Conclusion: Derivatives of the interpolated profiles showed that locations of IPs and 50% isodose points coincide.

© 2019 Greater Poland Cancer Centre. Published by Elsevier B.V. All rights reserved.

* Corresponding author.

E-mail addresses: nsarigul@hacettepe.edu.tr (N. Sarıgül), yagiz.yedekci@hacettepe.edu.tr (F.Y. Yedekçi), yeginer@hacettepe.edu.tr (M. Yeğiner), hakyol@hacettepe.edu.tr (F. Akyol), utku@hacettepe.edu.tr (H. Utku).

<https://doi.org/10.1016/j.rpor.2019.10.008>

1507-1367/© 2019 Greater Poland Cancer Centre. Published by Elsevier B.V. All rights reserved.

1. Aim

This study aimed to analyze the CyberKnife dose profile for the location of IPs and to determine the appropriate normalization procedure to ensure that the recommended dose is delivered correctly.

2. Background

Medical Physicists define the IP of a dose profile curve as the point of the curve where progression of dose deposition changes direction geometrically from positive to negative or vice versa. Because at that point, the normal vector to the profile curve changes its direction from one side to the opposite; the curve crosses its tangent line at IP.

Historically, significance of the IP of a dose profile stems from the fact that the dose characteristics of linear accelerators (linacs) without a flattening filter are very different from those of linacs with an FF. While FFs produce a uniform intensity across the field, the FFF dose profile is not uniform but peaked.¹ Physical and dosimetric differences between flattened and unflattened dose profile raised concerns about the conventional normalization applied to the dose profiles of unflattened beams. In order to allow dose profiles from FFF beam to be realistically compared to dose profiles from FF beams, a normalization factor based on IP was proposed by Pönisch et al.² They introduced a normalization factor for the Varian Clinac 21EX system, defined as the ratio of the dose at the IP of the penumbral region of the unflattened profile to the dose at the IP of the flattened profile, multiplied by the dose value at the central axis of the flat profile. Renormalization allowed them to evaluate the field size at IPs, or at 50% dose level to keep the common dosimetric field size definition. Mesbahi et al.³ calculated the dosimetric features of an unflattened 6-MV photon beam of an Elekta SL-25 linac using the Monte Carlo (MC) method. They employed the method of Pönisch et al. for penumbra comparisons between flattened and unflattened cases, and used some features of beam profiles, such as the penumbra between off-axis doses of 80% and 20% and the location of the field edge at an off-axis dose of 50%. Sinha et al.⁴ investigated the penumbra of a 6-MV flattened beam and a 7-MV unflattened beam of a Siemens Artiste Linac using the IP method. Pichandi et al.⁵ aimed to analyze physical parameters of FFF beams and determined the IP for standardizing beam flatness and penumbra for Varian True Beam system. They defined the radiation (dosimetric) field size as the lateral separation between IPs along the central axis and proposed a method to find its location. In a more recent study, dimensions of radiation fields delivered by eight dosimetrically matched Varian iX linacs were determined.⁶ In their conclusion, emphasis was put on the difficulty and importance of maintaining radiation field size consistency between “matched” linacs.

The above-mentioned analyses of FFF beams were based on the establishment of a relationship between standard FF and FFF beams. Relationship applies mainly to linacs that have both the standard FF and FFF beams. On the other hand, the CyberKnife system does not use an FF beam. Therefore,

validity of IP definition for the field size has to be investigated for the CyberKnife system. It is known that accurate measurements of dose distributions play an indispensable role in the success of field size determination. Importance of accurately measuring and reporting field sizes was emphasized by several authors.^{6–8} One way to evaluate the dosimetric accuracy is to compare detector measurements and to compare them with MC simulation. In this study, as part of quality assurance, we first used the gamma evaluation method to quantitatively compare dose profiles measured with different detectors and with reference MC calculated profiles. The comparison was performed using different acceptability criteria. Finally, the location of IPs on dose profiles of the CyberKnife system and dosimetric field sizes was determined.

3. Materials and methods

3.1. Detectors

We used two real-time detectors: a microDiamond (PTW 60019, PTW, Freiburg, Germany) and a diode SRS detector (PTW 60018). The microDiamond detector had a 1 μm -thick, 1.1 mm-radius circular active layer and a sensitive volume of 0.004 mm³. The disk-shaped Diode SRS detector had a radius of 0.6 mm and a sensitive volume of 0.3 mm³. These detectors have a high spatial resolution, a small and stable background, and fast acquisition. Both are useful when small-step measurements in a high-gradient region are needed.

3.2. Irradiation procedure

The CyberKnife system uses interchangeable circular secondary collimators, the field sizes of which are defined under an isocentric setup. All irradiations were performed using CyberKnife 6 MV with various collimation sizes from 15 mm to 60 mm. The microDiamond and Diode SRS detectors were placed in a water tank. The measurement step between each point for all cone sizes was 0.2 mm. Beam profiles for all collimators were measured at a depth of 5 cm with Source-to-Axis Distance (SAD) of 80 cm. All profiles were normalized to a maximum dose in the central axis at a depth of 5 cm. Dose measurements at 200 MU/measurement were repeated three times.

3.3. EGSnrc Monte Carlo simulations

Monte Carlo techniques are widely accepted as the gold standard for radiation transport simulation in radiation therapy.^{9,10} Dose profiles were calculated using EGSnrc/BEAMnrc Monte Carlo code^{11,12} in conjunction with the DOSXYZnrc code. Phase space files for 15, 20 30, and 60 mm cones were generated using a model of the treatment head of the CyberKnife SRS system¹³ and the phase space data were stored below the secondary collimator. The histories of 3×10^8 electrons incident on the target were simulated. The mean energy of the incident electrons and the full width at half-maximum (FWHM) of the electron radial intensity distribution were 6.7 MeV and 3.2 mm, respectively.¹³ The global electron and photon cut-off energies (ECUT and PCUT)

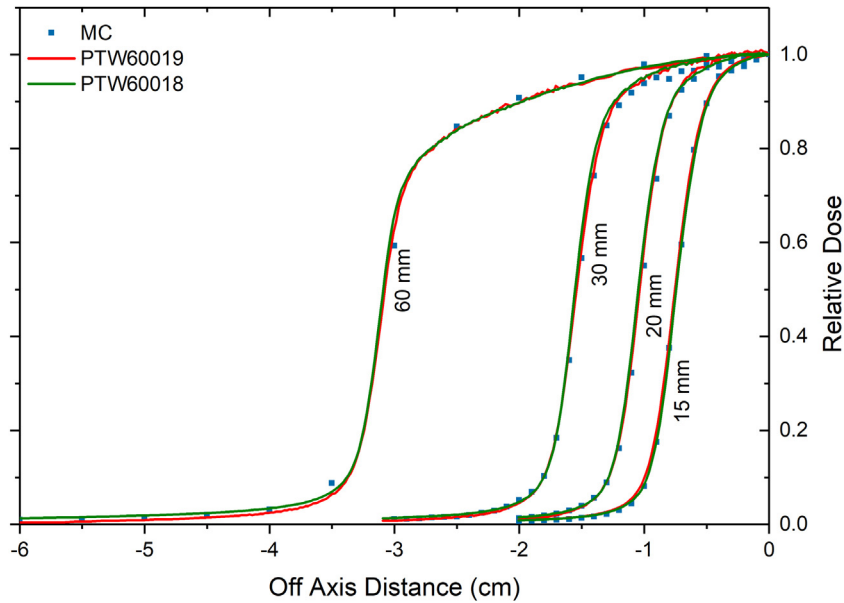


Fig. 1 – Beam profiles corresponding to 15, 20, 30 and 60 mm cone sizes. The blue square for MC, green and red lines are for Diode SRS and microDiamond, respectively.

for particle transport were set to 700 keV (total energy) and 10 keV, respectively. The phase space data were used as a source for DOSXYZnrc. The MC simulation was validated through percentage depth dose (PDD) and output factors measurements and results were published elsewhere.¹⁴

For MC dose profiles the water phantom was modelled as $30\text{ cm} \times 30\text{ cm} \times 30\text{ cm}$ using different voxel sizes, 1 mm for all cone sizes except 60 mm cone for which it was 5 mm. The dose profile computation was at the depth of 5 cm with SAD of 80 cm. With these specifications, 1×10^7 – 3×10^8 histories were needed to achieve a statistical uncertainty less than 1%.

3.4. Gamma evaluation method

To establish an acceptance criterion between different dosimeter readings, gamma index of the evaluation method,^{15,16} $\gamma(\vec{r}_r, \vec{r}_m)$, was used to quantitatively compare reference (MC calculated) and measured dose profiles:

$$\gamma(\vec{r}_r, \vec{r}_m) = \sqrt{\frac{|\vec{r}_m - \vec{r}_r|^2}{\Delta r^2} + \frac{|D(\vec{r}_m) - D(\vec{r}_r)|^2}{\Delta D^2}} \quad (1)$$

where Δr is the predetermined spatial difference (distance-to-agreement) between the dose point \vec{r}_m in the measured dose distribution and the nearest point \vec{r}_r in the reference dose distribution containing the same dose value; $D(\vec{r}_r)$ and $D(\vec{r}_m)$ are doses at reference and measured locations, respectively; and ΔD is the predetermined dose difference at those locations. Gamma evaluation takes into account acceptability of both the percentage dose ($\Delta D\%$) and the spatial difference (Δr in mm) to compare two different dose distributions. The comparison passes if $\gamma \leq 1$.

4. Results

Dose profiles from data measured with a microDiamond detector, a Diode SRS detector and those calculated using the MC simulation are shown in Fig. 1. For smaller cones, the dose distribution had a steeper decline in the penumbral region, which shows that the measurements need to be made in small steps. This requires the use of dosimeters with small sensitive volumes because a small change in the position of a detector in the penumbral region results in a large difference in dose readings. For all cone sizes, the differences in detector measurements were $<2\%$ in the central and penumbral regions.

Gamma evaluation was applied to measurements from all detectors and the MC calculation, for all cone sizes, and the results were compared. The acceptability criteria define the permissible range of variation in acceptability based on clinical requirements and measurement limitations. In Fig. 2a–c, gamma indexes are presented for the 15 mm cone. Shown values serve as a measure of disagreement or agreement in the locations that fail or pass the acceptability criteria, respectively. For three chosen acceptability criteria based on previously gained experience,¹⁷ Fig. 2a shows the distribution of gamma indexes to determine locational agreements between Diode SRS measurements and the reference dose distributions which was calculated by EGSnrc software tool using MC method. In Fig. 2b, locational agreements are shown for microDiamond measurements and MC. Comparison of measurements with MC computed doses via gamma evaluation method with criterion of (3%, 0.5 mm) are in good agreement at all locations. When comparison is made between Diode SRS and microDiamond as shown in Fig. 2c, we observe similar results. Values of gamma index with acceptance criteria of either (1%, 1 mm) or (2%, 0.2 mm) were greater or equal to 1 ($\gamma \geq 1$) within the region where dose ratios were in the range

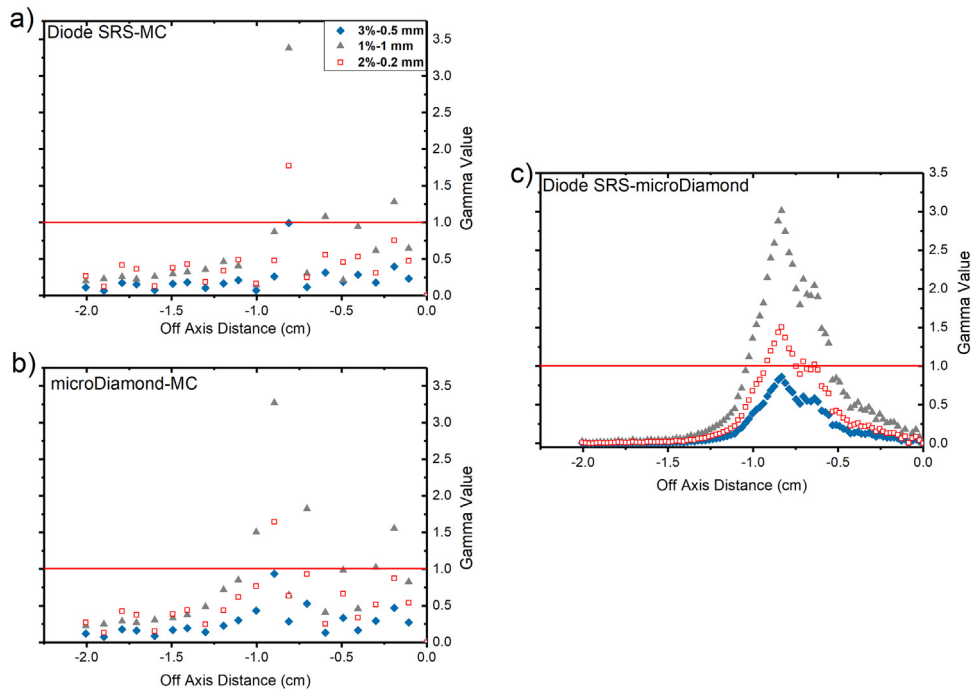


Fig. 2 – Gamma values for three different sets of tolerance criteria (3%–0.5, 1%–1, 2%–0.2). Comparison test for (a) Diode SRS measurements and MC method (b) microDiamond measurements and MC method (c) microDiamond measurements and Diode SRS.

of 10 to 90% across the dose profile. (3%, 0.5 mm) criterion was satisfied at all locations.

Several authors^{18,19} have already emphasized the importance of measurements with fine steps and the use of smaller detectors within the penumbra region. In Eq. (1), the variables \bar{r}_r and \bar{r}_m are controllable because they are adjustable in MC calculations and measurements, respectively. Using the smallest step to advance a detector within the penumbral region yields the smallest difference between two successive dose measurements. This should allow tighter acceptance criteria. However, Fig. 2 shows that even when the smallest step size (0.2mm) was used in the experiment, the acceptance criteria of (2%, 0.2mm) did not yield $\gamma \leq 1$ at most locations. The combination of 3% dose difference criterion and 3 mm spatial difference (the distance-to-agreement) criterion is commonly used as the acceptability criteria for the gamma evaluation method.^{17,20} In this study, the gamma index criterion $\gamma \leq 1$ can be satisfied throughout the profile when the dose difference and the distance-to-agreement criteria are set to 3% and 0.5 mm, respectively. For the 6MV photon beam of the CyberKnife, the distance between the 20% and 80% isodoses in the penumbral is about ≤ 3 mm at a phantom depth of 5 cm. Therefore, the level of uncertainty involved in determining the field edge and the dosimetric accuracy introduced as a result can easily be ascertained.

Since the CyberKnife system does not use an FF, the standardization procedure of LINAC systems working both with and without FF is not applicable. We used the cubic spline interpolation technique to locate the IPs. Because the IP is the location where the second derivative of a function describing

Table 1 – Dosimetric field sizes (FWHM) obtained by detectors and MC computation.

Cone Size (mm)	Dosimetric field size (mm)		
	PTW 60019	PTW 60018	MC
60	61.3	61.3	61.4
30	30.5	30.6	30.6
20	20.3	20.3	20.4
15	15.1	14.6	15.4

the dose profile is zero, the first and second derivatives of the dose profiles were determined using the profiles interpolated from the step by step measurements for the diamond and diode detectors. Fig. 3 shows the dose profiles measured using microDiamond detector and their first and second derivatives for the 15 and 60 mm cones. For all the cones in this study, the maximum of first derivatives of dose profiles are at the 50% isodose points and values of second derivatives are zero at those locations. The first and second derivative plots show that the 50% dose points coincide with the IP of the profile. This result holds for all fields examined in this study.

Table 1 gives the dosimetric field sizes determined at a phantom depth of 5 cm by each detector for each cone size. The voxel size for the calculated dose distributions was approximately the same as the sensitive size of both SRS diode and microDiamond detectors. This is important in order to make the measurements consistent with calculations. Depending on the type of detector used, there may be differences in the field size determinations. In Table 1, the lowest relative difference between the dosimetric and geometric field size is 0.7% for the 15 mm cone from the microdiamond measurement.

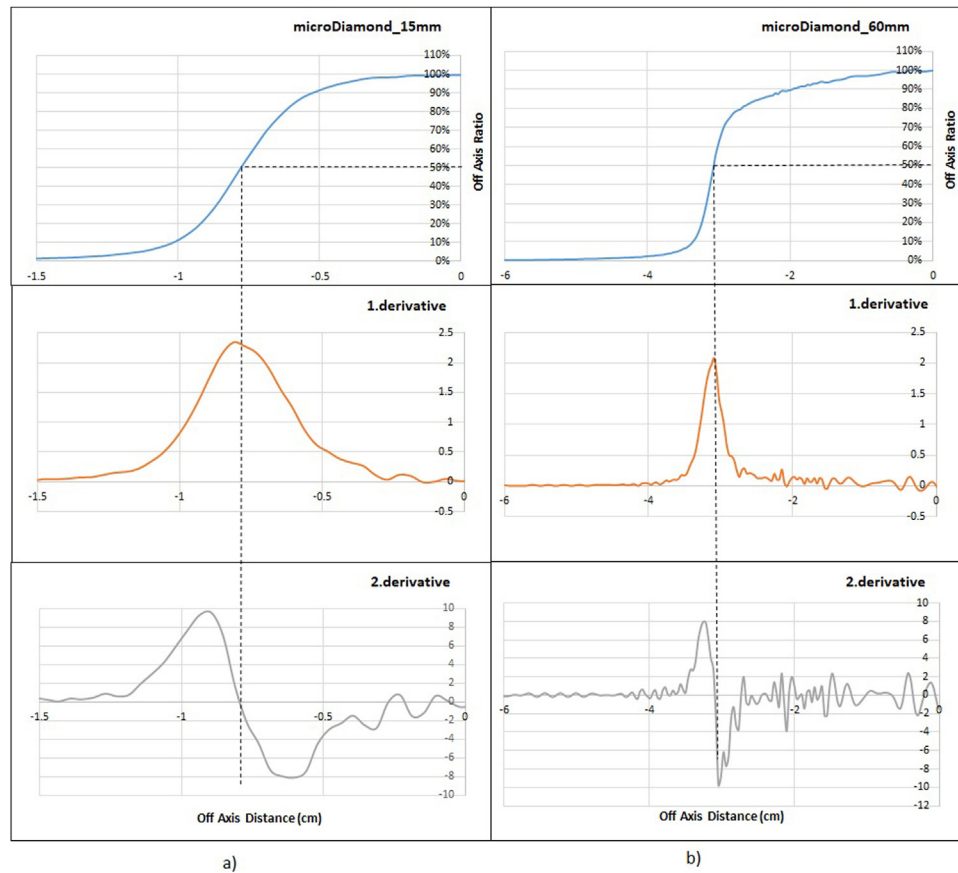


Fig. 3 – Column on the left shows the dose profile using microdiamond (a) for 15 mm cone, and its first and second derivate obtained by interpolation right column is (b) for 60 mm cone.

5. Discussion

In this work, the microDiamond detector, the Diode SRS detector and EGSnc Monte Carlo model for CyberKnife SRS System were used to measure off-axis profiles of 1560 mm diameter radiosurgical beams of a CyberKnife robotic SRS system. Dose profiles were then compared using the gamma index $\gamma(\bar{r}_r, \bar{r}_m)$ of the evaluation method given by Eq. (1). Results of MC dose calculations were used as reference in the evaluation of the gamma index. In general, a standard MC dose calculation accuracy better than 2% is considered acceptable. In our case, MC history was chosen to achieve a statistical uncertainty less than 1%.

The gamma evaluation method is a combination between the dose difference and the distance-to-agreement evaluation methods. Our calculations showed that although we obtained less than 2% difference in detector measurements, a looser criterion on the dose difference should be selected to pass the comparison test with the MC calculation. It is important to evaluate both the spatial difference and the dose difference to satisfy requirements on both geometrical and dosimetrical precision together.

Referred publications in the Introduction section classify unflattened profiles based on the IPs rather than the conventional full width half maximum (FWHM, 50% dose level). In the CyberKnife system, the nominal field size for the FFF beam

is defined by a collimator setting. In general, variation in a profile is measured along two orthogonal axes (in 2D measurements) within the field and the maximum variation is defined. Therefore, Pichandi et al.⁵ have defined dosimetric field size for FFF beams through lateral separation between IPs along the central axis. When characteristics of a beam is such that the 50% dose edges and IPs are at the same location on the beam profile, two outcomes become apparent. First, normalization using the dose at inflection points or the re-normalization procedure described by Fogliata et al.¹⁸ is not necessary. Secondly, the linac system in operation can locate the maximum variation in the profile much faster, making it easier to determine the variation along the two orthogonal axes.

For all cone sizes, we found that first derivatives have peaks at the location of 50% dose edge. Second derivative curves change their signs while passing through the 50% dose edge and the value of second derivative functions are zero at that point. In Fig. 3, we present the results for the largest and the smallest cones. It can be seen from the figure that the IP in the unflattened profile and the 50% dose edge are at the same locations. Beam characterization involves measurement of the dose profile and the dose profile analysis allows to understand the beam's characteristics. The location of IPs on a dose profile is one of the beam properties that remains unchanged for a given linac, regardless of which cone size is used to deliver the dose. Therefore, in order to show the validity of IP locations

on profiles, it is sufficient to determine its locations between 60 mm and 15 mm cones.

According to the vendor's specification, both SRS diode and the microdiamond are well suited for measurements in small fields less than 1 cm × 1 cm. Their length is exactly the same. Both are non-shielded and do not show a volume effect. Volume effect is especially important because it causes penumbra broadening (FWHM). SRS diode cross section in the beam is slightly smaller than for the microdiamond detector. The water-equivalent window thickness of the microdiamond is smaller; however, the difference between their correction factors we obtained for another study was not significant.¹⁴ In this work, measured values for field sizes were the same except for the 15 mm cone. For the smallest cone, there is a direction of difference between these two evaluations. This may be attributed to the decrease in the sensitivity of SRS diode when the contribution of the scattered photons to the absorbed dose becomes lower as the field size becomes smaller. In summary, the microDiamond and Diode SRS showed similar performance for 20–60 mm cones. For 15 mm cone, however, the microDiamond had a reasonably better performance.

6. Conclusion

In this study, a comparative test for acceptability of dose profile measurements using different detectors was made with respect to EGSnrc Monte Carlo calculation. Analysis by the gamma evaluation method showed that detector measurements were acceptable within (3%, 0.5 mm) dose and distance intervals, respectively.

In some studies,^{2–5} radiation field size of FFF beam was defined through lateral separation between IPs along the central axis. In order to determine dosimetric field sizes, we also investigated the location of IPs on dose profiles. We revealed that the 50% isodose and the IPs are at the same location on the dose profile of 6 MeV CyberKnife system. This evaluation was done with the interpolation of the measured dose profile. Location of IP were determined by the first and second derivative methods. Measurements were carried out using very small measurement steps and the detectors are carefully positioned in order to attain the highest accuracy.

Ethical approval

This article does not contain any studies with human participants or animals performed by any of the authors.

Conflict of interest

None declared.

Financial disclosure

Some experimental data used in this study are from a scientific project that was funded by the Scientific and

Technological Research Council of Turkey (TÜBİTAK) (Grant contract no. 114S753).

Acknowledgement

We thank to Professor Fujio Araki for providing the numerical model of the Cyberknife for the MC computation.

REFERENCES

- Georg D, Knöös T, McClean B. Current status and future perspective of flattening filter free photon beams. *Med Phys* 2011;**38**(3):1280–93, <http://dx.doi.org/10.1118/1.3554643>.
- Pönisch F, Titt U, Vassiliev ON, Kry SF, Mohan R. Properties of unflattened photon beams shaped by a multileaf collimator. *Med Phys* 2006;**33**(6):1738–46, <http://dx.doi.org/10.1118/1.2201149>.
- Mesbahi A, Mehnati P, Keshtkar A, Farajollahi A. Dosimetric properties of a flattening filter-free 6-MV photon beam: a Monte Carlo study. *Radiat Med* 2007;**25**(7):315–24, <http://dx.doi.org/10.1007/s11604-007-0142-6>.
- Sinha SN, Yadav G, Ashokkumar S, Raman K, Thiyagarajan R, Mishra M. Penumbra width calculation for flattening filter free beam 7MV and flattened beam 6MV using inflection point. Fifty-fourth annual meeting of the American Association of Physicists in Medicine. *Med Phys* 2012;**39**(6):3712, <http://dx.doi.org/10.1118/1.4735098>.
- Pichandi A, Ganesh KM, Jerin A, Balaji K, Kilara G. Analysis of physics parameters and determination of inflection point for flattening filter free beams in medical linear accelerator. *Rep Pract Oncol Radiother* 2014;**19**:322–31, <http://dx.doi.org/10.1016/j.rpor.2014.01.004>.
- Kairn T, Asena A, Charles PH, et al. Field size consistency of nominally matched linacs. *Australas Phys Eng Sci Med* 2015;**38**(2):289–97, <http://dx.doi.org/10.1007/s13246-015-0349-2>.
- Cranmer-Sargison G, Charles PH, Trapp JV, Thwaites DI. A methodological approach to reporting corrected small field relative outputs. *Radiation Oncol* 2013;**109**(3):350–5, <http://dx.doi.org/10.1016/j.radonc.2013.10.002>.
- Das JJ, Ding GX, Ahnesjö A. Small fields: nonequilibrium radiation dosimetry. *Med Phys* 2008;**35**(1):206–15, <http://dx.doi.org/10.1118/1.2815356>.
- Raynaert N, Van der Mark SC, Schaart DR, et al. Monte Carlo treatment planning for photon and electron beams. *Radiat Phys Chem* 2007;**76**(4):643–86, <http://dx.doi.org/10.1016/j.radphyschem.2006.05.015>.
- Seco J, Verhaegen F. *Monte Carlo Techniques in Radiation Therapy*. Taylor & Francis Group, CRC Press; 2013. p. 342.
- Nelson R, Hirayama H, Rogers DWO. *The EGS4 Code System Stanford Linear Accelerator Center Report SLAC-265*. Stanford, CA: SLAC; 1985.
- Rogers DWO, Faddegon BA, Ding GX, Ma CM, Wei JS, Mackie TR. BEAM: a Monte Carlo code to simulate radiotherapy treatment units. *Med Phys* 1995;**22**:503–24, <http://dx.doi.org/10.1118/1.597552>.
- Araki F. Monte Carlo study of a CyberKnife stereotactic radiosurgery system. *Med Phys* 2006;**33**:2955, <http://dx.doi.org/10.1118/1.2219774>.
- Akyol F, Sarigul N, Yeginer M, Yedekci Y, Utku H. Evaluation of NanoDot optically stimulated luminescence dosimeter for cone-shaped small field dosimetry of CyberKnife stereotactic radiosurgery unit: a Monte Carlo simulation and dosimetric verification study. *J Med Phys* 2019;**44**(1):27–34, <http://dx.doi.org/10.4103/jmp.JMP.96.18>.

15. Low DA, Harms WB, Mutic S, Purdy JA. A technique for the quantitative evaluation of dose distributions. *Med Phys* 1998;25(5):656–61, <http://dx.doi.org/10.1118/1.598248>.
16. Shiu AS, Tung S, Hogstrom KR, et al. Verification data for electron beam dose algorithms. *Med Phys* 1992;19:623–36, <http://dx.doi.org/10.1118/1.596808>.
17. Van Dyk J, Barnett RB, Cygler JE, Shragge PC. Commissioning and quality assurance of treatment planning computers. *Int J Radiat Oncol Biol Phys* 1993;26:261–73, [http://dx.doi.org/10.1016/0360-3016\(93\)90206-B](http://dx.doi.org/10.1016/0360-3016(93)90206-B).
18. Fogliata A, Garcia R, Knöös T, et al. Definition of parameters for quality assurance of flattening filter free (FFF) photon beams in radiation therapy. *Med Phys* 2012;39(10):6455–64, <http://dx.doi.org/10.1118/1.4754799>.
19. Aspradakis MM. Small Field MV Photon Dosimetry. World Congress on Medical Physics and Biomedical Engineering. September 7-12, Munich, Germany. 2009;44(103):854. https://doi.org/10.1007/978-3-642-03474-9_239.
20. Jiang SB, Sharp GC, Neicu T, Berbeco RI, Flampouri S, Bortfeld T. On dose distribution comparison. *Phys Med Biol* 2006;51:759–76, <http://dx.doi.org/10.1088/0031-9155/51/4/001>.